doi:10.1016/j.jmb.2011.06.019 J. Mol. Biol. (2011) xx, xxx–xxx

Contents lists available at www.sciencedirect.com

Journal of Molecular Biology

journal homepage: http://ees.elsevier.com.jmb

Rotations of the 2B Sub-domain of *E. coli* UvrD Helicase/Translocase Coupled to Nucleotide and DNA Binding

Haifeng Jia[1], Sergey Korolev[2]*, Anita Niedziela-Majka[1], Nasib K. Maluf[1], George H. Gauss[1], Sua Myong[3], Taekjip Ha[4,5], Gabriel Waksman[6] and Timothy M. Lohman[1]*

[1]*Department of Biochemistry and Molecular Biophysics, Washington University School of Medicine, 660 South Euclid Avenue, St. Louis, MO 63110, USA*
[2]*Department of Biochemistry and Molecular Biology, St. Louis University School of Medicine, St. Louis, MO 63104, USA*
[3]*Department of Bioengineering, University of Illinois, Urbana-Champaign, IL 61801, USA*
[4]*Department of Physics and Center for the Physics of Living Cells, University of Illinois, Urbana-Champaign, IL 61801, USA*
[5]*Howard Hughes Medical Institute, Urbana, IL 61801, USA*
[6]*Institute of Structural and Molecular Biology, Birkbeck and University College London, Malet Street, London WC1E 7HX, UK*

Received 8 March 2011;
received in revised form
6 June 2011;
accepted 13 June 2011

Edited by A. Pyle

Keywords:
DNA repair;
fluorescence;
FRET;
crystal structure;
allostery

Escherichia coli UvrD is a superfamily 1 DNA helicase and single-stranded DNA (ssDNA) translocase that functions in DNA repair and plasmid replication and as an anti-recombinase by removing RecA protein from ssDNA. UvrD couples ATP binding and hydrolysis to unwind double-stranded DNA and translocate along ssDNA with 3′-to-5′ directionality. Although a UvrD monomer is able to translocate along ssDNA rapidly and processively, DNA helicase activity *in vitro* requires a minimum of a UvrD dimer. Previous crystal structures of UvrD bound to a single-stranded DNA/duplex DNA junction show that its 2B sub-domain exists in a "closed" state and interacts with the duplex DNA. Here, we report a crystal structure of an apo form of UvrD in which the 2B sub-domain is in an "open" state that differs by an ~160° rotation of the 2B sub-domain. To study the rotational conformational states of the 2B sub-domain in various ligation states, we constructed a series of double-cysteine UvrD mutants and labeled them with fluorophores such that rotation of the 2B sub-domain results in changes in fluorescence resonance energy transfer. These studies show that the open and closed forms can interconvert in solution, with low salt favoring the closed conformation and high salt favoring the open conformation in the absence of DNA. Binding of UvrD to DNA and ATP binding and hydrolysis also affect the rotational conformational state of the

*Corresponding authors. E-mail addresses: korolevs@slu.edu; lohman@biochem.wustl.edu.
Present addresses: A. Niedziela-Majka, Gilead Sciences Inc., Foster City, CA 94404-1147, USA; N. K. Maluf, Department of Pharmaceutical Sciences, University of Colorado, Aurora, CO 80045, USA; G. H. Gauss, Department of Chemistry and Biochemistry, Montana State University, Bozeman, MT 59717, USA.

Abbreviations used: ssDNA, single-stranded DNA; SF1, superfamily 1; dsDNA, double-stranded DNA; FRET, fluorescence resonance energy transfer; BSA, bovine serum albumin; EDTA, ethylenediaminetetraacetic acid; PDB, Protein Data Bank.

Please cite this article as: Jia, H. *et al.*, Rotations of the 2B Sub-domain of *E. coli* UvrD Helicase/Translocase Coupled to Nucleotide and DNA Binding, *J. Mol. Biol.* (2011), doi:10.1016/j.jmb.2011.06.019

2B sub-domain, suggesting that 2B sub-domain rotation is coupled to the function of this nucleic acid motor enzyme.

Introduction

DNA helicases are nucleoside-triphosphate-hydrolyzing motor proteins that function in all aspects of DNA replication, recombination and repair that require formation of single-stranded DNA (ssDNA) intermediates.[1,2] Structurally, these enzymes can generally be grouped as either hexameric[3] or non-hexameric,[4] with the latter class having examples of functional monomers, dimers or filamentous oligomers.[2,5] These enzymes are also classified in different families or superfamilies based on conserved regions of primary structure,[6] with the superfamily 1 (SF1) and superfamily 2 classes being the largest.

Escherichia coli UvrD is a non-hexameric SF1 helicase and ssDNA translocase that functions in methyl-directed mismatch repair[7] and nucleotide excision repair[8] of DNA, reversal of replication forks[9,10] and replication of some plasmids.[11] UvrD also functions to remove proteins from DNA[12,13] and as an anti-recombinase by displacing RecA filaments from ssDNA intermediates, thus preventing homologous recombination.[14,15] In fact, these enzymes generally display multiple functions, including unwinding and strand separation of duplex DNA [or double-stranded DNA (dsDNA)] and translocation along ssDNA, as well as protein displacement from DNA.[16,17] Thus, it is likely that the helicase activity of these enzymes may not be their only function *in vivo*. In many cases, the different activities of these enzymes require different forms of the enzyme. For example, the monomeric forms of the SF1 enzymes, *E. coli* Rep, *E. coli* UvrD and *Bacillus stearothermophilus* PcrA, are all capable of rapid, highly processive and directional (3′ to 5′) translocation along ssDNA,[18–20] yet the monomeric forms are unable to unwind duplex DNA by themselves *in vitro*.[21–25] Either some self-assembly or interaction with an accessory factor is required to activate its helicase activity.[4,26]

The three SF1 helicases, *B. stearothermophilus* PcrA,[27,28] *E. coli* Rep[29] and *E. coli* UvrD,[30] are structurally similar (see Fig. 1), possessing a two-domain structure with each domain (1 and 2) being composed of two sub-domains (1A, 1B, 2A and 2B). ATP analogs bind between the 1A sub-domain and the 2A sub-domain, and ssDNA binds at the junction above the 1A and 2A sub-domains in the orientation shown in Fig. 1. Interestingly, two conformations of the Rep monomer ("closed" and "open" forms) were observed in the asymmetric unit of the Rep–ssDNA crystals.[29] The major difference between the two forms is the rotational configuration of the 2B sub-domain, which can rotate by ~130° about a hinge region connecting the 2B and 2A sub-domains. The apo[27] and 3′-ssDNA/dsDNA junction-bound[28] forms of the PcrA monomer also showed a large rotation of the 2B sub-domain by ~160°, with the apoenzyme having an open conformation and the DNA-bound form being in a closed conformation with the 2B sub-domain contacting the duplex DNA. Similarly, structures of a UvrD monomer bound to a 3′-ssDNA/dsDNA junction also show a closed orientation with the 2B sub-domain contacting the duplex region.[30] Single-molecule fluorescence resonance energy transfer (FRET) studies have shown that the 2B sub-domain of a Rep monomer is primarily in a closed conformation when bound to a 3′-ssDNA/dsDNA junction.[32]

The function of the 2B sub-domain is the subject of some debate. Based on the crystal structures of monomers of UvrD and PcrA bound to the 3′-ssDNA/dsDNA junctions,[28,30] it was suggested that the monomeric forms of these enzymes have processive helicase activity and that the interactions of the 2B sub-domain with the duplex region of the DNA junction are essential for helicase activity. However, there is substantial evidence that the monomeric forms of PcrA, UvrD and Rep are not processive helicases.[19,23,25,33] In fact, there is no evidence that the monomeric form of Rep can even initiate partial DNA unwinding.[21] Furthermore, removal of the Rep 2B sub-domain to form RepΔ2B monomer activates the helicase activity of the monomer, indicating that the 2B sub-domain in Rep is auto-inhibitory for monomeric helicase activity.[19] This suggests that the extensive 2B sub-domain–duplex DNA contacts inferred from the crystal structures of PcrA and UvrD monomers may not be important for their helicase activities. Rather, the 2B sub-domain may play a role in regulating the various activities of these enzymes through self-assembly or interactions with accessory proteins.[4] In fact, the rotational conformation of the 2B sub-domain may play a role in regulating its auto-inhibitory and other functions.

Here, we report a crystal structure of the apo form of UvrD that has its 2B sub-domain in an open conformation, indicating that the 2B sub-domain of UvrD, just as for Rep and PcrA, is capable of undergoing a similar large rotational conformational change. Using ensemble FRET studies, we show that the rotational conformational state of the 2B sub-domain of UvrD can be influenced by binding

Please cite this article as: Jia, H. *et al.*, Rotations of the 2B Sub-domain of *E. coli* UvrD Helicase/Translocase Coupled to Nucleotide and DNA Binding, *J. Mol. Biol.* (2011), doi:10.1016/j.jmb.2011.06.019

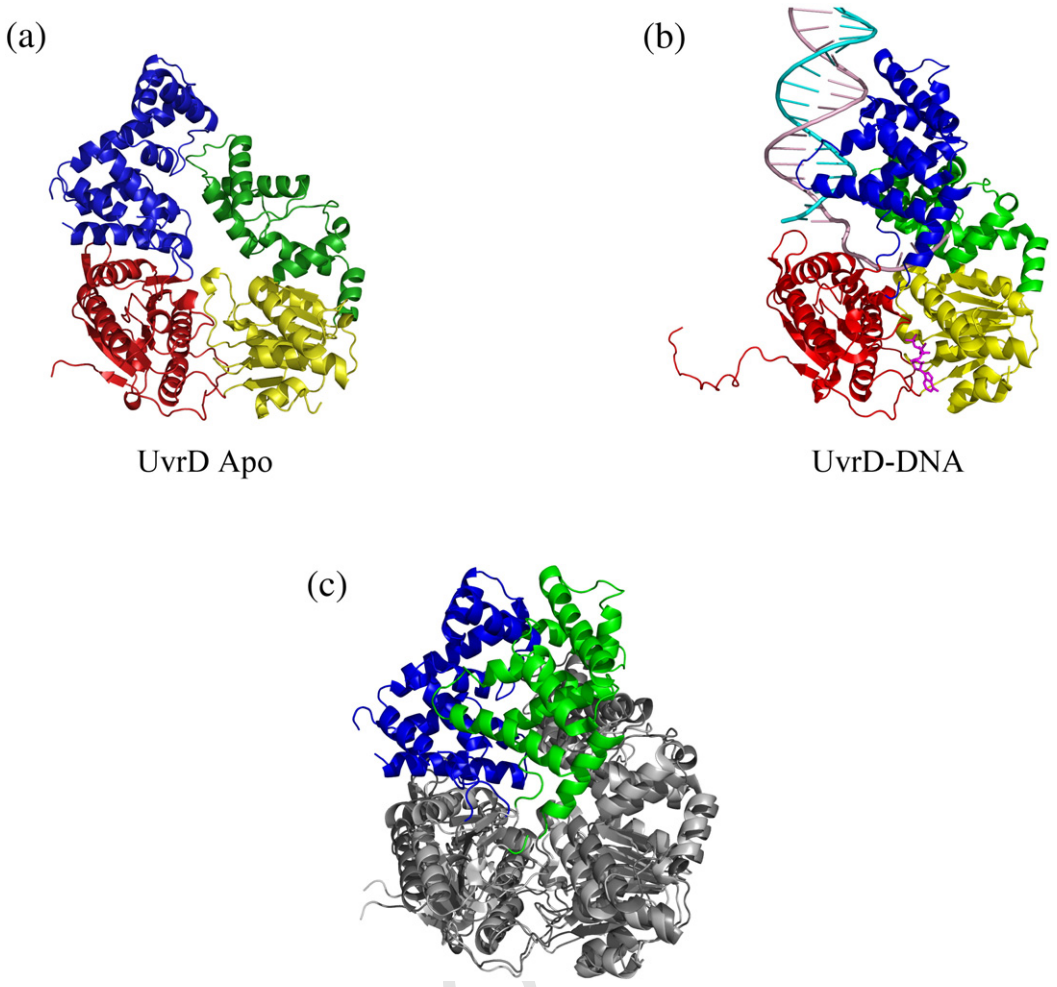

Fig. 1. Crystal structures of apo UvrD and a UvrD–DNA complex show that the 2B sub-domain can rotate to either an open or a closed conformation. Ribbon diagram representations of crystal structures of (a) apo UvrD (this report, PDB ID 3LFU) showing the 2B sub-domain in an open conformation and (b) UvrD bound to a 3′-ssDNA/duplex DNA junction[31] (PDB ID 2IS1) showing the 2B sub-domain in a closed conformation. Sub-domains 1A, 1B, 2A and 2B are colored yellow, green, red and blue, respectively. DNA in (b) is shown as a tubular model. The DNA strand with the 3′-ssDNA extension is colored light pink, and the partner strand is colored cyan. ATP analog AMPPNP is shown in sticks and colored magenta. (c) Sub-domains 1A, 1B and 2A of the two structures in (a) and (b) are superimposed, showing the difference in the rotational conformational states of the 2B sub-domains. Sub-domains 1A, 1B and 2A in UvrD structures are colored gray, and sub-domain 2B is colored green in the closed conformation and blue in the open conformation.

of ligands (e.g., nucleotides, DNA) and changes in solution conditions. The fact that rotational motion of the 2B sub-domain is coupled to the binding of nucleotides and DNA suggests that it is likely to be functionally important for some activities of this enzyme and/or their regulation.

Results

Apo UvrD structure

Crystal structures of a monomer of *E. coli* UvrDΔ40, UvrD with the last 40 aa deleted from its C-terminus, bound to a series of short 3′-ssDNA/dsDNA junctions have been reported by Lee and Yang.[30] In all of these structures, one of which is depicted in Fig. 1b, the 2B sub-domain (blue) of UvrD is in a closed orientation, relative to the 1B sub-domain (green). In this orientation, the 2B sub-domain contacts the 1B sub-domain, and these two sub-domains bind the duplex region of the DNA junction. This orientation is similar to the closed orientation observed in one of the structures of *E. coli* Rep bound to ssDNA [$(dT)_{16}$].[29] In the open structure of Rep also bound to $(dT)_{16}$, the 2B sub-domain has rotated by ~130° about a hinge region connected to the 2A sub-domain, and there is no interaction between the 1B sub-domain and the 2B sub-domain.[29]

Please cite this article as: Jia, H. *et al.*, Rotations of the 2B Sub-domain of *E. coli* UvrD Helicase/Translocase Coupled to Nucleotide and DNA Binding, *J. Mol. Biol.* (2011), doi:10.1016/j.jmb.2011.06.019

We have determined a crystal structure to 1.8 Å of an apo form of a UvrDΔ73 monomer (residues 1–647) in which 73 aa have been deleted from its C-terminus. This UvrD mutant was used because this region of the C-terminus is not visible in the crystal structures of Rep and, thus, is likely unstructured and/or flexible. Deletion of these 73 aa also increased its solubility significantly. This mutant retains ATPase activity and monomeric ssDNA translocation activity [158 ± 8 nucleotides/s compared to wild-type monomer (191 ± 3 nucleotides/s[20])] as well as helicase activity (~30% of wild type with UvrDΔ73 in large molar excess over DNA).

In the UvrDΔ73 apo structure, the conformations of the 1A and 2A sub-domains are nearly identical with those in the open form of PcrA (1PJR) and the open Rep–ssDNA and the UvrD–DNA complexes (2IS1), with an rmsd of 1.3 Å among the 360 C^{α} atoms of the 1A and 2A sub-domains of the open and closed UvrD forms (Fig. 1c). There is a small rotation of the 1B sub-domain upon comparison of the open and closed UvrD structures, resulting in movement of the apical part (residue 360) by 8 Å.

The 2B sub-domain in the apo UvrD structure is in an open conformation, relative to the other three sub-domains (1A, 2A and 1B) (Fig. 1a). It rotates by nearly 160°, moving from one side of the 1B sub-domain in the open apo form to the opposite interface of the 1B sub-domain in the closed DNA-bound form (Fig. 1c). The magnitude of this 2B swiveling is very similar to that observed upon comparison of the apo PcrA structure[27] and its DNA complexes.[28] Importantly, the ssDNA and dsDNA binding sites are partially blocked in the UvrD and PcrA open forms (see Discussion). A large swiveling of the 2B sub-domain of an SF1 helicase was first observed in the crystal structure of two monomers of Rep bound to ssDNA [$(dT)_{16}$];[29] however, the magnitude of the Rep 2B sub-domain swiveling is smaller (~130°), and the 2B sub-domain does not block ssDNA binding to the 2A sub-domain, as is the case in the UvrD and PcrA open conformations. Overall, three different rotational conformations of the 2B sub-domain have been observed in various crystal structures of Rep, UvrD and PcrA. These include the open and closed forms of UvrD and PcrA, which are stabilized by extensive contacts with the 1B sub-domain and, thus, may represent stable conformations. The third is the open ssDNA-bound Rep form in which the ssDNA binding site is fully accessible. To examine the transitions among these conformational states further, we wished to probe the conformational changes in the 2B sub-domain in solution and upon binding different ligands.

Double UvrD mutant construction and fluorophore labeling

We used FRET to study 2B sub-domain rotation in solution. For this, we mutated three different amino acids (two at a time) in UvrD to Cys for subsequent labeling with donor and acceptor fluorophores. One mutated position (A473C) is within the 2B sub-domain, while the other positions are located in either the 1B sub-domain (A100C) or the 2A sub-domain (A370C) (Fig. 2a). Each position is exposed on the surface of UvrD, enabling convenient fluorescent labeling. Two different double-Cys mutants were constructed, UvrDΔCys[A100C, A473C] (referred to as DM-1B/2B) (Fig. 2b) and UvrDΔCys[A370C, A473C] (referred to as DM-2A/2B) (Fig. 2c). These mutations were made within an otherwise Cys-less UvrD protein, UvrDΔCys (see Materials and Methods). These positions are highlighted in the closed and open conformations of the UvrD structure in Fig. 2. DM-1B/2B was designed to yield a high FRET signal when 2B is in its closed conformation and a low FRET signal when 2B is in its open conformation (Fig. 2b), whereas DM-2A/2B was designed to observe a low FRET signal with 2B in its closed conformation and a high FRET signal with 2B in its open conformation (Fig. 2c).

UvrD(DM-1B/2B) and UvrD(DM-2A/2B) were labeled stochastically with an equimolar mixture of Cy3 (donor) and Cy5 (acceptor) maleimides (see Supplemental Materials). The average labeling efficiencies per protein were 85% for Cy3 and 92% for Cy5. The ssDNA-stimulated steady-state ATPase activity was reduced by about 25% for the labeled UvrD mutants compared to wtUvrD (data not shown). In addition, DNA unwinding activities of the labeled mutants were within 22% of those of wtUvrD (data not shown). The kinetics of ssDNA translocation of the monomeric UvrD double mutants were similar to those of wtUvrD monomers. Figure 3a–c show the time courses of ssDNA translocation for unlabeled UvrD(DM-1B/2B), wtUvrD and double-labeled UvrD(DM-1B/2B), respectively, for a series of different ssDNA lengths [$(dT)_{54}$, $(dT)_{79}$ and $(dT)_{104}$] labeled with fluorescein at the 5′ end. These single-round experiments monitor the quenching of fluorescein fluorescence upon arrival of a translocating UvrD monomer at the 5′ end followed by UvrD dissociation from DNA and trapping by heparin.[20,34] The macroscopic translocation rate determined from a global non-linear least-squares analysis of the unlabeled UvrD (DM-1B/2B) monomer time courses is 182 ± 8 nucleotides/s, which is the same within error as the rate for the wtUvrD monomer (191 ± 3 nucleotides/s) under the same conditions.[20] The translocation rate for the double-labeled UvrD(DM-1B/2B) monomer is slightly slower (155 ± 10 nucleotides/s).

The 2B sub-domain rotational conformation is sensitive to salt concentration and type

Superposition of the apo UvrD crystal structure reported here and the UvrD–DNA crystal

Please cite this article as: Jia, H. et al., Rotations of the 2B Sub-domain of E. coli UvrD Helicase/Translocase Coupled to Nucleotide and DNA Binding, J. Mol. Biol. (2011), doi:10.1016/j.jmb.2011.06.019

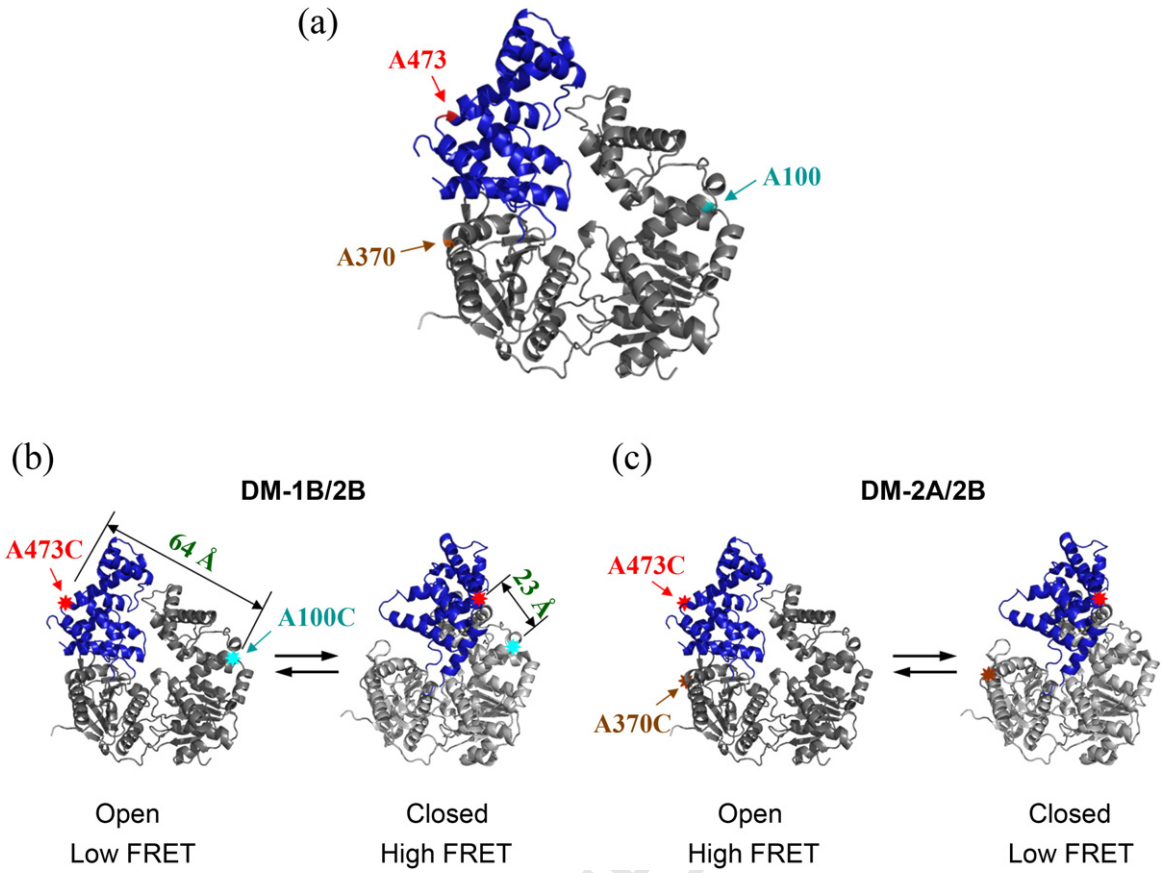

Fig. 2. Design and fluorescent labeling of the UvrD mutants used to monitor the 2B sub-domain rotation by FRET. Two different double-Cys UvrD mutants, UvrDΔCys[A100C, A473C] (DM-1B/2B) and UvrDΔCys[A370C, A473C] (DM-2A/2B), were made by the substitution of alanine with cysteine at the indicated positions. (a) The positions of the three Ala-to-Cys mutations are indicated in the apo UvrD structure. (b) UvrD(DM-1B/2B) labeled with a mixture of Cy3 and Cy5 should show high FRET in the closed form and low FRET in the open form. The distances between A100C and A473C in the two conformations are also indicated. (c) UvrD(DM-2A/2B) labeled with a mixture of Cy3 and Cy5 should show low FRET in the closed form and high FRET in the open form.

structures[31] (Fig. 1c) indicates that the 2B sub-domain can undergo an ~160° rotation about a hinge region connected to the 2A sub-domain. To determine whether the 2B sub-domain orientation could be influenced by solution conditions, we first examined the relative fluorescence of Cy3 donor and Cy5 acceptor in ensemble FRET studies of Cy3/Cy5-labeled UvrD mutants DM-1B/2B and DM-2A/2B as a function of [NaCl] in the absence of DNA. These experiments were carried out in 10 mM Tris–HCl (pH 8.3 at 25 °C) and 20% (v/v) glycerol [100 μg/ml bovine serum albumin (BSA) was included to reduce protein sticking to the cuvette]. Figure 4 shows fluorescence emission spectra for the Cy3/Cy5-labeled UvrD DM-1B/2B mutant at different NaCl concentrations from 20 mM to 600 mM. In these experiments, the Cy3 donor fluorescence was excited at 515 nm, and both donor (Cy3) and acceptor (Cy5) fluorescence emissions were monitored. For the DM-1B/2B mutant, the donor fluorescence emission intensity increases, while the acceptor fluorescence intensity decreases concomitantly as the [NaCl] is increased, as shown in Fig. 5a. Since we show below that these fluorescence changes are due only to FRET, the decrease in FRET observed for the DM-1B/2B mutant indicates that the 2B sub-domain moves from a relatively closed orientation to a more open conformation as the [NaCl] increases. Similar experiments performed with the Cy3/Cy5-labeled DM-2A/2B mutant (Fig. 5b) show the opposite effect, namely, a decrease in donor fluorescence intensity and an increase in acceptor fluorescence intensity as the [NaCl] is increased, which is expected for this mutant if the 2B sub-domain swivels open as the [NaCl] increases. Thus, the two UvrD mutants, DM-1B/2B and DM-2A/2B, give qualitatively consistent results, indicating that the 2B sub-domain of a UvrD monomer is able to freely rotate in solution and that it moves from a

Please cite this article as: Jia, H. *et al.*, Rotations of the 2B Sub-domain of *E. coli* UvrD Helicase/Translocase Coupled to Nucleotide and DNA Binding, *J. Mol. Biol.* (2011), doi:10.1016/j.jmb.2011.06.019

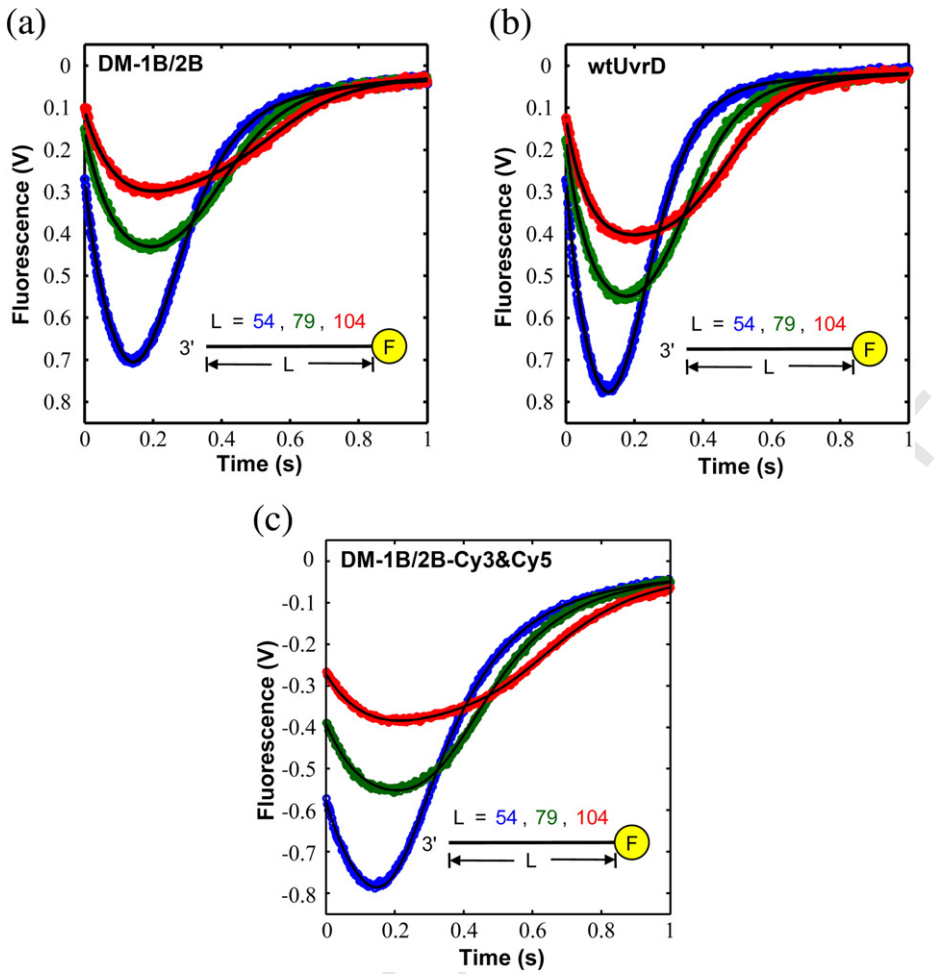

Fig. 3. ssDNA translocation kinetics of UvrD(DM-1B/2B) and wtUvrD monomers. Kinetics of UvrD monomer translocation along $(dT)_{54}$ (blue), $(dT)_{79}$ (green) and $(dT)_{104}$ (red) were examined by monitoring the decrease in fluorescein fluorescence accompanying the arrival of UvrD at the 5′ end of fluorescein-labeled ssDNA, followed by an increase in fluorescence upon dissociation of the UvrD translocase. ssDNA translocation kinetics of (a) UvrD(DM-1B/2B) monomer (not labeled with Cy3 and Cy5), (b) wtUvrD monomer and (c) UvrD(DM-1B/2B) monomer (labeled with Cy3 and Cy5). The continuous lines are simulated time courses using the best-fit parameters from a global nonlinear least-squares analysis of the data, as described previously.[20] UvrD (25 nM, postmixing) was preincubated with 5′-F-$(dT)_L$ (50 nM, postmixing) in buffer T_{20}, and translocation was initiated with the addition of ATP (0.5 mM), $MgCl_2$ (2 mM) and heparin (4 mg/ml) (all final concentration) at 25 °C.

closed to a more open conformation as the [NaCl] increases.

To determine whether the fluorescence changes plotted in Fig. 5a and b are due solely to FRET changes, we compared all four transitions (acceptor and donor for both DM-1B/2B and DM-2A/2B) directly in Fig. 5c by replotting them so that all normalized donor and acceptor changes are shown as increasing from zero to one. As is clear in Fig. 5c, three of the transitions [donor and acceptor for UvrD(DM-1B/2B) and donor for UvrD(DM-2A/2B)] are nearly identical, with a midpoint of ~65 mM NaCl, whereas the acceptor transition for UvrD(DM-2A/2B) is offset to higher [NaCl] (midpoint of ~120 mM NaCl). Since the donor and acceptor fluorescence changes observed for UvrD(DM-1B/2B) mutant are quantitatively anti-correlated, these changes appear to be due solely to FRET effects. However, although the donor and acceptor fluorescence changes for the UvrD(DM-2A/2B) mutant show qualitative anti-correlation, they differ quantitatively, suggesting that some fluorescence changes other than FRET occur for the Cy5 acceptor fluorescence in UvrD(DM-2A/2B).

We infer that this non-FRET effect is due to DM-2A/2B molecules that are labeled with the Cy5 acceptor at position 370 within the 2A sub-domain for two reasons. First, it is not likely due to molecules labeled with Cy5 in the 2B sub-domain, since the same labeling position was used for the

Please cite this article as: Jia, H. *et al.*, Rotations of the 2B Sub-domain of *E. coli* UvrD Helicase/Translocase Coupled to Nucleotide and DNA Binding, *J. Mol. Biol.* (2011), doi:10.1016/j.jmb.2011.06.019

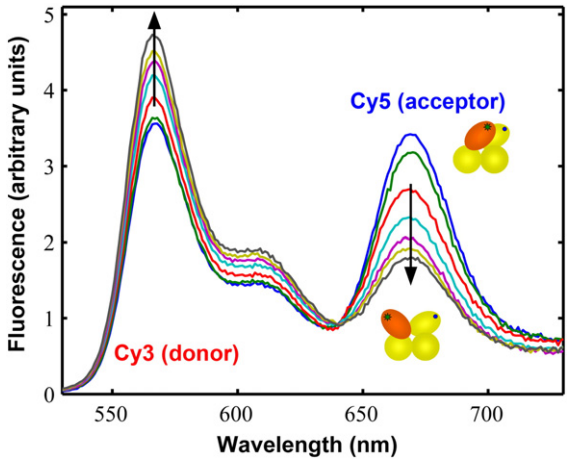

Fig. 4. Cy3/Cy5 FRET changes accompany rotation of the 2B sub-domain of UvrD(DM-1B/2B). Cy3 (donor)-labeled and Cy5 (acceptor)-labeled UvrD(DM-1B/2B) (20 nM) in 10 mM Tris–HCl (pH 8.3 at 25 °C) and 20% (v/v) glycerol was titrated with concentrated NaCl in the same buffer. The fluorescence emission spectra of labeled UvrD(DM-1B/2B) (excitation at 515 nm) are plotted at several [NaCl]. The arrows indicate the increase in fluorescence intensity of Cy3 (donor) and the concomitant decrease in fluorescence of Cy5 (acceptor) with increasing [NaCl], demonstrating the transition from a closed 2B sub-domain conformation to an open conformation. The cartoons showing the relative orientation of the four sub-domains are colored yellow for sub-domains 1A, 1B and 2A and orange for sub-domain 2B.

DM-1B/2B protein for which the results suggest that all fluorescence changes are due to FRET. Second, since the Cy3 donor fluorescence transition of DM-2A/2B overlays quantitatively with both the donor and the acceptor transitions observed with DM-1B/2B, the changes in donor (Cy3) fluorescence would appear to be due only to FRET changes. Hence, we surmise that the Cy5 fluorescence of DM-2A/2B molecules labeled with Cy5 at the Cys370 position within the 2A sub-domain is either quenched or enhanced additionally when the 2B sub-domain is in either the closed or the open conformation. Based on the position of amino acid 370, it seems most likely that the problem occurs when the 2B sub-domain is in the open conformation, since the 2B sub-domain comes in close proximity to A370 (see Fig. 2a). In any event, because of this, all remaining experiments reported here were performed with the DM-1B/2B mutant, since the fluorescence changes that occur with both donor and acceptor fluorophores appear to be due solely to FRET changes and, thus, result from true distance changes, at least for the monomeric apo UvrD. However, our experiments with both mutants support the qualitative conclusion that the 2B domain swivels to a more open conformation at high salt and that the open and closed forms are in equilibrium in solution. In the absence of single-molecule studies, we cannot conclude whether the salt-induced transition represents gradual changes in the rotational conformation of the 2B sub-domain or changes in the relative population of two or a few conformational states.

We have further examined the origins of the effect of salt on the 2B sub-domain orientation by comparing the effects of a series of other salts (KCl, NaBr, $NaCH_3CO_2$ and $MgCl_2$) on the closed-to-open transition. We find that all salts induce the transition; however, the midpoints of the transitions are sensitive to the type of cation and anion (Supplementary Fig. S1). These results indicate that the salt-induced transition to the open form observed here is accompanied by the direct binding of both cations and anions and is not due to a simple screening effect of ionic strength. Examination of the UvrD–DNA crystal structure in the closed form shows a number of potentially important electrostatic interactions between charged groups of sub-domains 1B and 2B that could explain these salt effects. A pair of salt bridges (D115–K389 and D118–R396) appear to be capable of forming between 1B and 2B. There are also several positively charged residues in sub-domain 1B (R121, K124, R125, K128 and R183) and negatively charged residues in sub-domain 2B (D404, E408, D420, D424 and D432). Since these residues are far apart in the open state, it makes sense that high salt would favor the open conformation.

In the UvrD crystal structures, the α-carbons of the two cysteines at positions 473 (2B) and 100 (1B) in UvrD(DM-1B/2B) are separated by 64 Å for the apo UvrD in the open conformation and 23 Å when UvrD is in the closed conformation in the UvrD–DNA structure (see Fig. 2b). Examination of the UvrD crystal structures indicates that the open form in the UvrD apo structure and the closed form in the UvrD–DNA structure[31] represent the extremes of the possible rotational states that the 2B sub-domain can occupy; hence, further rotations are not possible. Thus, it is not possible that the low-salt plateau FRET value corresponds to a 2B rotational state in which Cys473 and Cy100 are closer together than in the UvrD–DNA crystal structure. Thus, we assume that the orientation of the 2B sub-domain in the high-NaCl-concentration plateau region corresponds to the open form of the apo crystal structure (Fig. 1a) and that the low-NaCl-concentration plateau region corresponds to the closed form of the UvrD–DNA crystal structure (Fig. 1b). We can then use the Förster equation assuming $R_0 = 54$ Å for the Cy3/Cy5 pair[35] (see Materials and Methods) to infer distance changes from the FRET changes that we observe in the DNA and nucleotide binding experiments described below. Alternatively, we could assume that the high- and low-salt plateaus correspond to the apo form of UvrD in solution and

Please cite this article as: Jia, H. *et al.*, Rotations of the 2B Sub-domain of *E. coli* UvrD Helicase/Translocase Coupled to Nucleotide and DNA Binding, *J. Mol. Biol.* (2011), doi:10.1016/j.jmb.2011.06.019

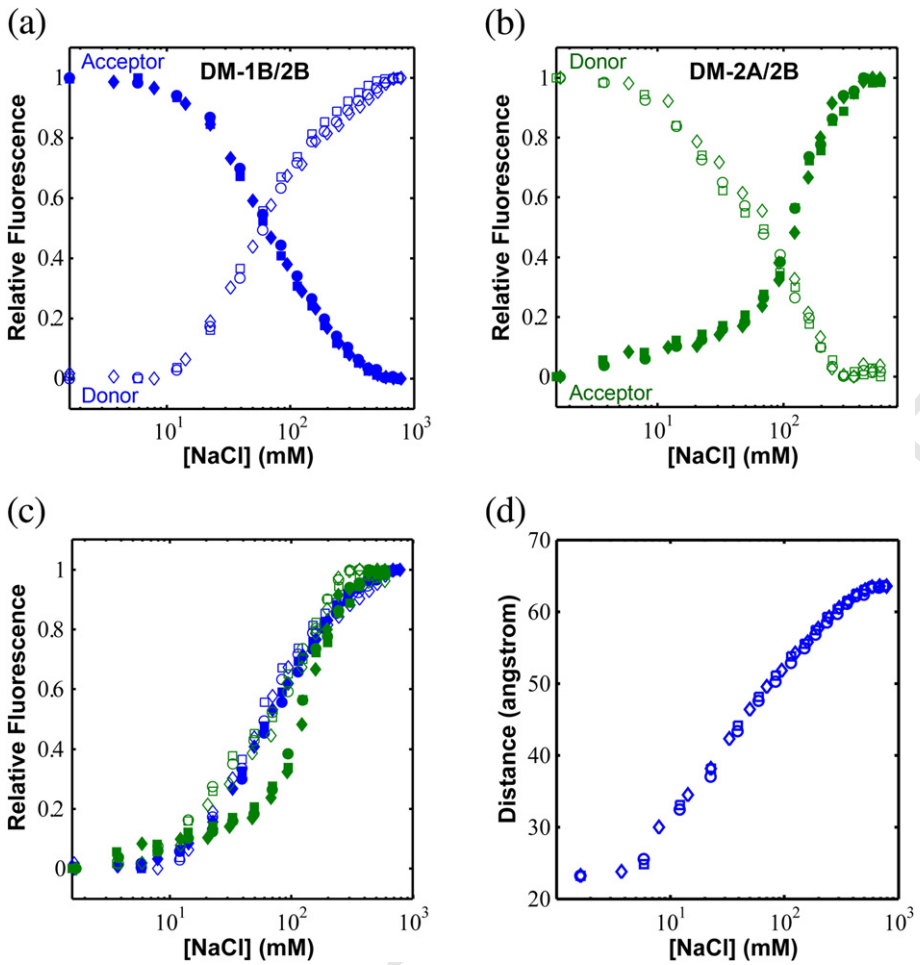

Fig. 5. NaCl concentration influences the 2B sub-domain rotational conformation. Normalized fluorescence changes in donor (open symbols, excitation at 515 nm/emission at 566 nm) and acceptor (filled symbols, excitation at 515 nm/emission at 670 nm) for (a) UvrD(DM-1B/2B) labeled with Cy3/Cy5 and (b) UvrD(DM-2A/2B) labeled with Cy3/Cy5. For each, three experimental data sets are shown (squares, circles and diamonds). (c) Replot of the donor and acceptor signals for DM-1B/2B and DM-2A/2B so that all normalized donor and acceptor changes are shown as increasing from zero to one. (d) The FRET changes were used to calculate distances between the FRET pairs for UvrD(DM-1B/2B) as a function of [NaCl]. The distances between the two alanines (A100 and A473) in the crystal structures of the open (apo) and closed[31] conformations shown in Fig. 1 were used to calibrate the end points of the titrations.

the UvrD–DNA structure in solution, respectively. However, this assignment seems less reasonable since, as we show below, the FRET value of the UvrD–DNA complex is near the midpoint of the high- and low-salt transitions.

UvrD binding to ssDNA induces opening of the 2B sub-domain

We next used UvrD(DM-1B/2B) to examine whether DNA binding affects the rotational orientation of its 2B sub-domain. These experiments were performed in buffer T_{20} including BSA (100 μg/ml), and thus, before the addition of DNA, the 2B sub-domain of UvrD is near its fully closed low [NaCl] conformation, although not completely closed (~35 Å *versus* ~23 Å in the fully closed conformation). Figure 6a shows that, upon addition of saturating concentrations of $(dT)_{35}$ (500 nM as shown in Fig. 6b) to DM-1B/2B (20 nM), the Cy3 (donor) fluorescence increases while the Cy5 (acceptor) fluorescence decreases, indicating that binding of $(dT)_{35}$ induces an opening of the 2B sub-domain of UvrD (to ~50 Å), although not as fully open as at high [NaCl] (~64 Å). Figure 6b shows the relative donor and acceptor fluorescence changes accompanying a full titration of DM-1B/2B with $(dT)_{35}$. The normalized forms of these two transition curves (Fig. 6c) are identical, suggesting that the FRET changes result only from distance changes. The titration curve with $(dT)_{70}$ is similar (data not shown).

Please cite this article as: Jia, H. *et al.*, Rotations of the 2B Sub-domain of *E. coli* UvrD Helicase/Translocase Coupled to Nucleotide and DNA Binding, *J. Mol. Biol.* (2011), doi:10.1016/j.jmb.2011.06.019

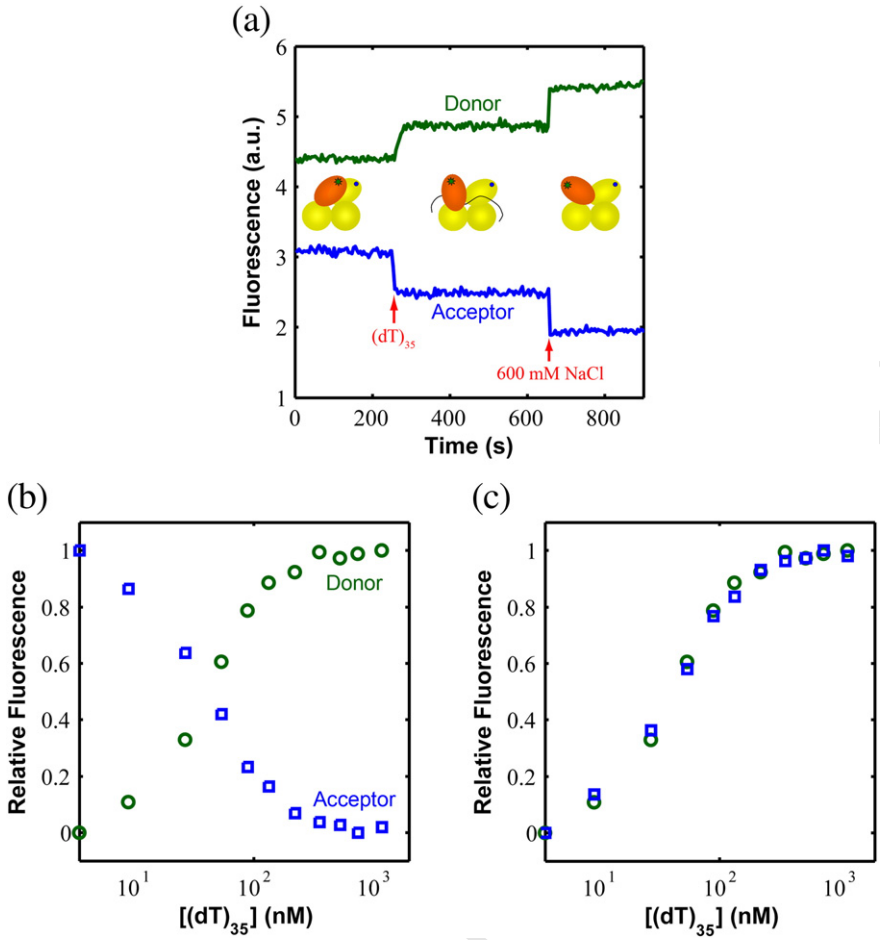

Fig. 6. Binding of UvrD to ssDNA induces opening of the 2B sub-domain. (a) Changes in the donor and acceptor signals when 500 nM $(dT)_{35}$ and 600 mM NaCl are added to 20 nM DM-1B/2B. The final signal at 600 mM NaCl is used as a control since, under this condition, the 2B sub-domain is fully open. (b) The relative Cy3 (donor) and Cy5 (acceptor) fluorescence intensities of DM-1B/2B (20 nM) upon titration with $(dT)_{35}$ in buffer T_{20}. The fluorescence signal increases for the donor and decreases for the acceptor until saturation is reached, indicating a relative opening of the 2B sub-domain upon binding $(dT)_{35}$. (c) Replot to normalize the donor and acceptor changes as increasing from zero to one, indicating that all fluorescence signal changes upon binding $(dT)_{35}$ result from FRET changes due to distance changes.

Binding of UvrD to duplex DNA with a 3′-ssDNA tail induces 2B sub-domain opening

When saturating amounts (50 nM) (Supplementary Fig. S2) of an ssDNA/duplex DNA junction (18-bp duplex) with a 20-nucleotide 3′ tail are added to UvrD(DM-1B/2B) in buffer T_{20}, the donor signal increases, and the acceptor signal decreases, indicating that UvrD binding to this DNA also causes the 2B sub-domain to become more open (Fig. 7a). When saturating amounts of a partial duplex with a short 3′-ssDNA tail is added, UvrD(DM-1B/2B) shows relatively little FRET change, indicating that the 2B sub-domain remains mostly in the closed form. It therefore appears that the 2B sub-domain adopts a partially open conformation when bound to an ssDNA/duplex DNA junction in solution, not fully closed as is observed in the UvrD–DNA junction crystal structures (see Fig. 1b).[30] As DNAs with longer ssDNA tails are examined (at saturating concentrations), the degree of 2B sub-domain opening increases with the largest change observed for ssDNA lengths larger than 25 (Fig. 7b).

ATP binding and hydrolysis are coupled to swiveling of the 2B sub-domain of UvrD

To further investigate the functional significance of the 2B sub-domain movement, we measured FRET changes within UvrD(DM-1B/2B) upon binding ATP and nucleotide analogs that mimic some of the reaction intermediates during the ATP hydrolysis cycle. Figure 8 shows the results of ensemble FRET experiments performed with DM-1B/2B in the presence of saturating concentrations of $(dT)_{35}$ (500 nM) and several different nucleotides

Please cite this article as: Jia, H. *et al.*, Rotations of the 2B Sub-domain of *E. coli* UvrD Helicase/Translocase Coupled to Nucleotide and DNA Binding, *J. Mol. Biol.* (2011), doi:10.1016/j.jmb.2011.06.019

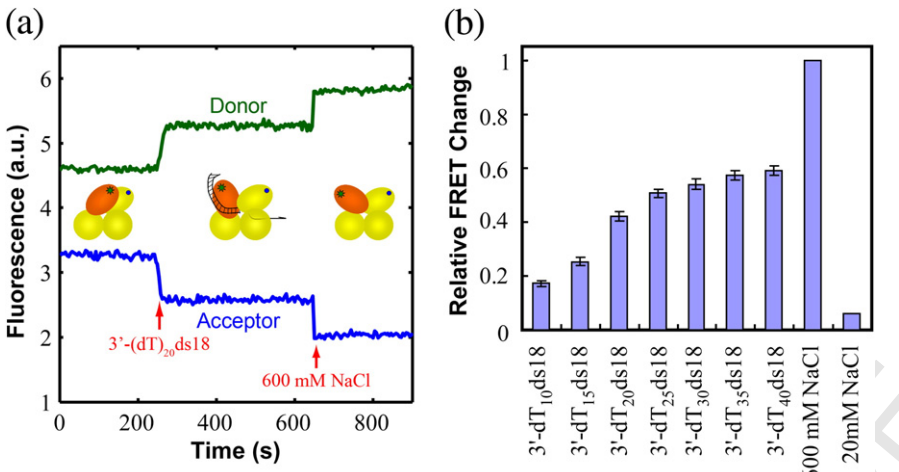

Fig. 7. Binding of a partial DNA duplex with a 3′-ssDNA tail promotes 2B sub-domain opening. (a) An increase in Cy3 (donor) fluorescence and a decrease in Cy5 (acceptor) fluorescence occur upon binding a 3′-ssDNA/duplex DNA junction (50 nM) and addition of 600 mM NaCl to DM-1B/2B (20 nM). (b) Relative FRET changes indicate an opening of the 2B sub-domain as the length of the 3′-ssDNA tail of the partial duplex increases from 10 to 40 nucleotides. The FRET signals at low [NaCl] (20 mM) and high [NaCl] (600 mM) are used as references, respectively.

in buffer T_{20}. The relative FRET change, as well as, by inference, the 2B sub-domain conformation, is at an intermediate position between fully open (600 mM NaCl) and closed (20 mM NaCl) when bound to ssDNA alone and remains nearly the same upon further binding of ATP or ADP (Fig. 8a, c and d). However, the FRET signal change is considerably reduced when ATPγS (a slowly hydrolyzable ATP analog) or ADP·MgF_3 (which is believed to mimic an ADP–inorganic phosphorus intermediate)[36] is added with the ssDNA (Fig. 8b–d). Therefore, the nucleotide ligation state has a clear effect on the average rotational conformational state of the UvrD 2B sub-domain. These results suggest that the 2B sub-domain of a UvrD monomer exists predominantly in several partially open conformations in all of these ligation states when bound to ssDNA. Thus, the 2B sub-domain of a UvrD monomer likely moves among a series of partially open states during ATP-driven ssDNA translocation. Movement of the 2B sub-domain is clearly modulated by interactions with DNA, as well as by ATP binding and hydrolysis.

Discussion

We report a crystal structure of a monomeric apo form of *E. coli* UvrD with its 2B sub-domain in an open conformation. Previous crystal structures of a UvrD monomer bound to a series of 3′-ssDNA/duplex DNA junctions show the 2B sub-domain in a quite different closed conformation.[30] Thus, the 2B sub-domain of a UvrD monomer can exist in both an open form and a closed form (differing by a rotation of ~160°), similar to what has been observed for the structurally similar *E. coli* Rep[29] and *B. stearothermophilus* PcrA SF1 monomers.[27,28] We also show, using ensemble FRET studies, that the open and closed forms can interconvert in solution and that the rotational conformational state of the 2B sub-domain is sensitive to the salt concentration as well as to anion and cation type, with low salt concentration favoring the closed conformation and high salt concentration favoring the open conformation in the absence of DNA. With increasing [NaCl], the 2B sub-domain rotates from a closed orientation to an open conformation with its maximum opening occurring near 600 mM NaCl, with a transition midpoint near 65 mM NaCl. The rotational conformational state of the 2B sub-domain is also affected by DNA binding as well as ATP binding and hydrolysis. In the previous structural studies of UvrD[31] and PcrA,[28] only the closed conformations were considered as the active forms of the enzyme. Within this closed form, small conformational changes corresponding to the opening and closing of the cleft between the 1A sub-domain and the 2A sub-domain upon ATP binding and hydrolysis were proposed to be coupled to translocation. The FRET experiments reported here suggest that binding of UvrD to ssDNA or partial duplex DNA induces swiveling of the 2B sub-domain, which adopts an intermediate state that is only partially open. Thus, the 2B sub-domain can populate intermediate rotational conformational states between the most open and the most closed states, and DNA binding and nucleotide binding affect the relative populations of these states.

The need for rotation of the 2B sub-domain can be understood, at least partially, by examining its conformations in the extreme closed and open states

Please cite this article as: Jia, H. *et al.*, Rotations of the 2B Sub-domain of *E. coli* UvrD Helicase/Translocase Coupled to Nucleotide and DNA Binding, *J. Mol. Biol.* (2011), doi:10.1016/j.jmb.2011.06.019

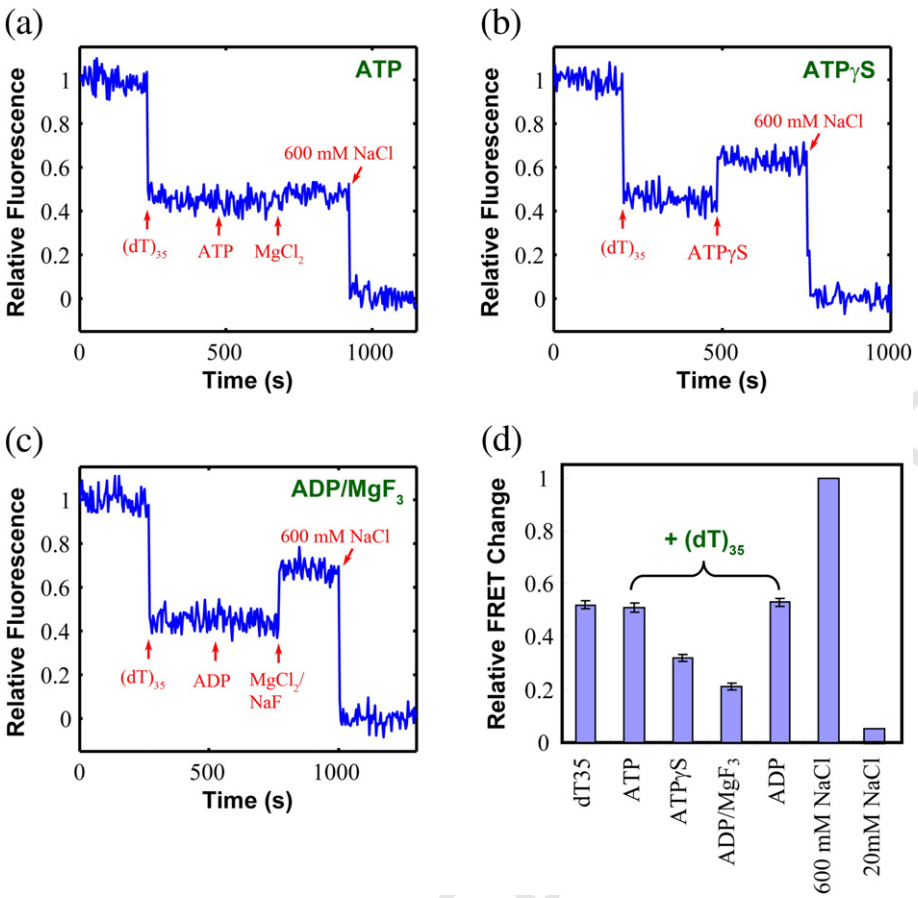

Fig. 8. ATP analogs affect the rotational conformation of the 2B sub-domain differently in the presence of ssDNA. The relative acceptor fluorescence of Cy3/Cy5-labeled UvrD(DM-1B/2B) (20 nM) is shown when interacting with (a) ATP, (b) ATPγS and (c)-ADP·MgF_3 in the presence of saturating concentration of $(dT)_{35}$. The arrows indicate the addition of 500 nM $(dT)_{35}$, 0.2 mM ATP, 0.5 mM $MgCl_2$, 600 mM NaCl, 0.2 mM ATPγS, 0.2 mM ADP and 0.5 mM $MgCl_2$/1.5 mM NaF, respectively. (d) The relative FRET signals reflecting different degrees of opening of the 2B sub-domain are compared in the presence of saturating concentration of $(dT)_{35}$ only, $(dT)_{35}$ + ATP, $(dT)_{35}$ + ATPγS, $(dT)_{35}$ + ADP·MgF_3, $(dT)_{35}$ + ADP and high/low salt (as references).

represented by the crystal structures of the UvrD–DNA complex and the apo UvrD, which either block the ssDNA binding site (closed form) or partially block the ssDNA and dsDNA binding sites (open form). Hence, movement of the 2B sub-domain away from these extreme conformations is needed to allow DNA binding. The relative orientations of the 2B sub-domains within the apo and DNA-bound forms of UvrD and PcrA as well as the two conformations of Rep when bound to ssDNA are illustrated in Fig. 9. The 2B sub-domain in the open structure of Rep is intermediate between the two extreme states, exemplified by the fully closed and open states observed for PcrA and UvrD. This intermediate state (Rep open state) is the only conformation among all of the UvrD, PcrA and Rep crystal structures in which both DNA binding sites (within the 1A and 2A sub-domains) appear to be fully accessible to ssDNA binding. In contrast, in the fully open forms of PcrA and UvrD, the ssDNA binding site of the 2A sub-domain appears partially blocked by the 2B sub-domain, and the dsDNA binding sites within the 2B and 1B sub-domains are involved in a 1B/2B interaction. In all of the closed forms, the ssDNA bound to the 1A sub-domain is completely occluded by the 1A, 1B and 2B sub-domains, suggesting that the initial binding of the 3′-ssDNA tail to the 1A sub-domain is likely to precede any closing of the 2B sub-domain. These results suggest that the conformation of the 2B sub-domain of UvrD may predominantly exist in a partially open form for most of its ATP cycle during ssDNA translocation. Only the ATP-bound (ATPγS or ADP·MgF_3) and fully unligated UvrD states exist in a more closed conformation in solution. This suggests that ADP or inorganic phosphorus release should induce a reopening of the 2B sub-domain, possibly allowing UvrD to translocate along ssDNA.

The FRET methods described here have previously been used to monitor rotational conformational

Please cite this article as: Jia, H. *et al.*, Rotations of the 2B Sub-domain of *E. coli* UvrD Helicase/Translocase Coupled to Nucleotide and DNA Binding, *J. Mol. Biol.* (2011), doi:10.1016/j.jmb.2011.06.019

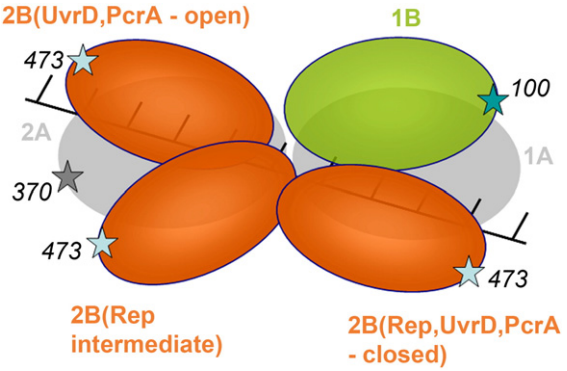

Fig. 9. Relative orientations of the 2B sub-domain in the crystal structures of the open and closed forms of UvrD, PcrA and Rep. The relative positions of the 2B sub-domains in the apo and DNA-bound forms of UvrD and PcrA compared with the positions of the 2B sub-domain in the open and closed conformations of Rep in complex with ssDNA. The six structures were compared by superimposing sub-domains 1A and 2A (shown in gray) and 1B (green) for all structures. The 2B sub-domains are in red. The positions of the fluorophores are also indicated. The closed conformations of UvrD, PcrA and Rep are similar, while the open conformation of Rep shows the 2B sub-domain in an intermediate position relative to the fully open conformations of UvrD and PcrA.

changes in the 2B sub-domains within Rep monomers[37] and PcrA monomers[33] during translocation along ssDNA. Single-molecule FRET studies of Rep[37] doubly labeled with Cy3/Cy5 showed that the 2B sub-domain of a Rep monomer closes gradually as the enzyme reaches a blockade that it cannot bypass (e.g., a duplex DNA region that the monomer cannot unwind). More recent single-molecule FRET studies of PcrA doubly labeled with Cy3/Cy5 showed that when PcrA initially binds the 5′-ssDNA/dsDNA junction, its 2B sub-domain adopts a closed conformation but then moves to a more open conformation and maintains the open conformation during ssDNA translocation that is coupled with repetitive ssDNA looping.[33] Those studies, as well as the results reported here, suggest that Rep, PcrA and UvrD monomers adopt a more open 2B sub-domain conformation during ssDNA translocation.

The FRET studies reported here suggest that, in solution, the fully closed conformation of UvrD is not highly populated when UvrD is bound to a 3′-ssDNA/dsDNA junction. In all UvrD–DNA crystal structures, the 2B sub-domain adopts a closed conformation, similar to the closed structure observed in the PcrA–DNA complexes.[28] However, our FRET results suggest that the 2B sub-domain adopts a partially open conformation when it interacts with the 3′-ssDNA/dsDNA junction in buffer T_{20}. The addition of DNA to UvrD(DM-1B/2B) induces an opening of the 2B sub-domain (Fig. 7a). However, when UvrD(DM-1B/2B) interacts with both the 3′-ssDNA/dsDNA and ATPγS (Mg^{2+}), the 2B sub-domain moves to a more closed conformation. In the ternary complex of UvrD–DNA–ADP·MgF_3, the 2B sub-domain moves to an even yet more closed conformation (data not shown), which is more consistent with the crystal structures of UvrD–DNA–AMPPNP and UvrD–DNA–ADP·MgF_3 ternary complexes.[31] Interestingly, while the 2B sub-domain also adopts a partially open conformation upon binding a 5′-ssDNA/dsDNA junction, it returns to a more closed conformation when ATP is added (data not shown). Further titration with Mg^{2+} causes a reopening of the 2B sub-domain (data not shown) as expected since, under these conditions, UvrD can initiate translocation along ssDNA from the junction in the 3′-to-5′ direction along the ssDNA tail.[38] When UvrD is bound to dsDNA alone, the 2B sub-domain closes even further relative to its position at 20 mM NaCl (data not shown), indicating that the ssDNA tails induce an opening of the 2B sub-domain.

It is not clear whether rotation of the 2B sub-domain is important for translocation or DNA unwinding is not known. It was shown previously that the 2B sub-domain of *E. coli* Rep inhibits the helicase activity of the Rep monomer *in vitro* and that removal of the 2B sub-domain to form RepΔ2B activates monomer helicase activity.[19,39] This suggests that the 2B sub-domain of Rep may play a role in regulating its activities.[19] In this regard, it is interesting that although both RepΔ2B and wtRep monomers can translocate rapidly along ssDNA with 3′-to-5′ directionality, removal of the 2B sub-domain increases the rate of ssDNA translocation of the RepΔ2B monomer by roughly 2-fold.[19] Hence, the 2B sub-domain of Rep modulates its rate of ssDNA translocation *in vitro*. As mentioned above, the open form of the 2B sub-domain of Rep observed in crystal structures is not in a fully open position compared to all of other UvrD and PcrA open structures. Furthermore, in this open Rep state, both DNA binding sites (1A and 2A sites) appear to be fully accessible to ssDNA binding. Since the 2B sub-domain partly blocks both ssDNA binding sites in the fully open and closed conformations of UvrD, our results suggest that, during ssDNA translocation, the 2B sub-domain of UvrD would be maintained in a partially open state, as has been observed for PcrA translocation.[33] The fact that the translocation rate for wtRep is slightly faster (about 50%) than that for wtUvrD[19,20] suggests the possibility that the fully open position of the 2B sub-domain in UvrD may inhibit translocation.

The focus of this study has been on the conformational changes that occur due to rotation of the 2B sub-domain of UvrD, an SF1 helicase/translocase. However, crystallographic studies of PcrA[28] and UvrD[31] suggest that ATP binding causes the cleft

Please cite this article as: Jia, H. *et al.*, Rotations of the 2B Sub-domain of *E. coli* UvrD Helicase/Translocase Coupled to Nucleotide and DNA Binding, *J. Mol. Biol.* (2011), doi:10.1016/j.jmb.2011.06.019

between the two RecA-like sub-domains 1A and 2A to close around the nucleotide and that the cleft reopens following ATP hydrolysis and ADP releasing and that this may drive ssDNA translocation.[2,40] Single-molecule FRET experiments also show that the interdomain cleft of the *Bacillus subtilis* DEAD box helicase YxiN closes upon binding both RNA and ATP, whereas it opens in the ADP-bound state.[41,42] Those movements are relatively small and, by themselves, would not cause the large FRET changes due to 2B sub-domain rotation that we report here. The experiments reported here and previous studies[33,37] suggest that rotational movement of the 2B sub-domain also occurs during ATP-driven ssDNA translocation.

Materials and Methods

Buffers and reagents

Buffers were prepared with reagent-grade chemicals using distilled water that was also deionized using a Milli-Q water purification system (Millipore Corp., Bedford, MA). Spectrophotometric-grade glycerol (99.5% purity) was from Aldrich (Milwaukee, WI). Buffer T_{20} is 10 mM Tris–HCl (pH 8.3 at 25 °C), 20 mM NaCl and 20% (v/v) glycerol. Storage buffer is 20 mM Tris–HCl (pH 8.3 at 25 °C), 200 mM NaCl, 50% (v/v) glycerol, 1 mM ethylenediaminetetraacetic acid (EDTA), 0.5 mM ethylene glycol bis(β-aminoethyl ether) *N*,*N*′-tetraacetic acid and 25 mM 2-mercaptoethanol. Storage minimal buffer is 20 mM Tris–HCl (pH 8.3 at 25 °C), 200 mM NaCl and 50% (v/v) glycerol. Buffer A is 20 mM Tris–HCl (pH 7.5 at 25 °C), 500 mM NaCl, 20% (v/v) glycerol and 5 mM 2-mercaptoethanol. Buffer B is 20 mM Tris–HCl (pH 7.5 at 25 °C), 500 mM NaCl and 20% (v/v) glycerol. Buffer C is 20 mM Tris–HCl (pH 8.3 at 25 °C), 20% (v/v) glycerol and 2 mM EDTA. ATP (Sigma-Aldrich) stock solutions were prepared in 50 mM NaOH (pH 7.5), and 500-μl aliquots were stored at −20 °C. ATP concentrations were determined spectrophotometrically using an extinction coefficient (259 nm) of 15.4×10^3 M^{-1} cm^{-1}.

Double-cysteine UvrD mutant plasmids

Site-directed mutagenesis was performed with the QuikChange kit (Stratagene, Cedar Creek, TX). Plasmids expressing all UvrD mutants were constructed by starting with plasmid pGG209, which contains the wtUvrD coding sequence cloned into plasmid pET-9d (kanamycin resistance and under the control of the T7 promoter; Novagen, Madison, WI). Mutations were first made to the DNA sequences encoding all six native cysteine residues in the UvrD gene (C52, C181, C322, C350, C441 and C640), replacing them with Ser in order to create a plasmid encoding a Cys-less UvrD plasmid Q4 (pGG209ΔCys). We did not anticipate this to be a problem for enzyme activity, since none of the naturally occurring Cys residues are conserved among UvrD, Rep and PcrA. The plasmid pGG209ΔCys was digested with restriction enzymes (NcoI and BstXI) and inserted with the PCR fragment amplified using primers AN55 and AN56 to generate an expression vector (pA10) to introduce a hexa-histidine (6×His) tag and thrombin cleavage site (MGSSHHHHHHSSGLVPRGSH, 20 aa) at the N-terminal end of the Cys-less UvrD mutant to aid in purification and labeling. Two different UvrD mutants, each containing two Cys residues, were then constructed, 6×His-UvrDΔCys[A100C,A473C] (called DM-1B/2B) and 6×His-UvrDΔCys[A370C, A473C] (called DM-2A/2B), by substituting Cys for Ala at the indicated positions within UvrDΔCys. Site-directed mutagenesis was carried out using plasmid pA10 and primers (AN70 and AN71 for A100C, AN72 and AN73 for A370C, AN74 and AN75 for A473C) to generate the plasmids expressing these double-cysteine mutants (named pA20 and pA21, respectively). All mutations were confirmed by DNA sequencing.

UvrDΔ73 protein expression and purification

A plasmid, pGG221, overexpressing UvrDΔ73 in which the last 73 C-terminal amino acids have been removed from UvrD was constructed as follows. The XbaI restriction fragment of pGG209 containing the wtUvrD coding region was ligated into the XbaI site of pET28a to generate plasmid pGG219. For removal of the DNA encoding the last 73 C-terminal amino acids from Ala648 on, primers were designed to replace the Ala648 codon with a stop codon (TAA), and the coding sequence after this position was deleted. Plasmid pGG219 was digested with XhoI and BsrGI to generate subclone 1. The C-terminal portion of pGG209 was amplified using the primers RSG-P4 and GHG72, digested with XhoI and BsrGI and ligated into subclone 1 to generate the UvrDΔ73 overexpression plasmid (called pGG221). All open reading frames were confirmed by DNA sequencing.

UvrDΔ73 protein under the control of the T7 promoter was overexpressed in strain *E. coli* BL21(DE3) ΔUvrD (with a deletion of wtUvrD gene, tetracycline resistant) and purified as described for wild-type UvrD[43] with the following modifications. First, the ssDNA cellulose column was loaded in buffer containing a lower [NaCl] (100 mM). Second, due to the C-terminal deletion, UvrDΔ73 did not show the usual extent of nuclease contamination as we find with wild-type UvrD; hence, the dsDNA cellulose column was not needed to remove the nuclease contamination. This suggests that the nuclease may interact with the unstructured C-terminus of UvrD.

Dna

The oligodeoxynucleotides used in this study were synthesized using an ABI model 391 (Applied Biosystems, Foster City, CA) and purified by electroelution of the DNA from denaturing polyacrylamide gels, as described previously.[44] The concentrations of the DNA strands were determined by spectrophotometric analysis of the mixture of mononucleotides after digestion of the DNA with snake venom phosphodiesterase I in 100 mM Tris–HCl (pH 9.2 at 25 °C) and 3 mM $MgCl_2$.[45] The oligodeoxynucleotides were dialyzed against 10 mM Tris–HCl (pH 7.5 at 25 °C) and stored at −20 °C. Duplex DNA was formed by annealing the top strand with an

Please cite this article as: Jia, H. *et al.*, Rotations of the 2B Sub-domain of *E. coli* UvrD Helicase/Translocase Coupled to Nucleotide and DNA Binding, *J. Mol. Biol.* (2011), doi:10.1016/j.jmb.2011.06.019

equal molar of complementary bottom strand in 10 mM Tris–HCl (pH 7.5 at 25 °C) plus 50 mM NaCl by heating to 95 °C for 5 min and then slowly cooling to room temperature over a period of 2 h. Duplex DNA formation was confirmed by native PAGE on 10% acrylamide gel in 1× Tris–borate–EDTA buffer.

UvrDΔ73 crystallization, data collection and refinement

Crystals of the UvrD C-terminal truncation UvrDΔ73 were obtained by the hanging-drop method. One microliter of protein solution, containing 30 mg/ml UvrDΔ73 in 20 mM Tris–HCl (pH 8.0), 0.1 M NaCl and 2 μM β-mercaptoethanol, was mixed with 1 μl of reservoir buffer, containing 0.1 M *N*,*N*-bis(2-hydroxyethyl)glycine 9.1, 1.0 M $(NH_4)_2SO_4$ and 2% polyethylene glycol 400. Crystals (~0.5 mm × 0.3 mm × 0.3 mm) were grown at room temperature in 1 week. They were gradually transferred into 3.0 M $(NH_4)_2SO_4$, 0.1 M *N*,*N*-bis(2-hydroxyethyl)glycine 9.1, 2% polyethylene glycol 400 and 5% glycerol and flash frozen at 100°K in a stream of nitrogen vapor.

Data were collected at beam line 19ID, Structural Biology Center, at Argonne National Laboratory and processed by HKL2000[46] program and truncated by CCP4 programs.[47] Reflections from three thin-resolution layers corresponding to weak ice rings were excluded from the data set. An initial solution was found by the molecular replacement method using the AMoRe program[48] and a polyalanine structure of PcrA helicase [Protein Data Bank (PDB) entry code 1PJR] as a search model. The molecular replacement solution was subjected to rigid-body refinement using the program CNS0.5[49] for the whole molecule and, subsequently, for each domain separately. The side chains and the loop regions were built in a few rounds in program O[50] using electron density maps calculated with $2F_o - F_c$ coefficient as well as simulated annealing omit maps. The structure was refined by a simulated annealing protocol with a maximum-likelihood target. Final refinement was performed with the program REFMAC,[51] and the parameters of refinement are shown in Table 1. Residues 1–2, 160–163, 521–525 and 542 were omitted due to lack of density, and residues 3, 157–168, 520, 526, 543, 545 and 547 were built as alanines because of poor density. Of the total number of residues, 92.7% are in the core of the Ramachandran plot, and 7.3% are in allowed regions. The coordinates were deposited into the PDB database (PDB ID 3LFU).

Table 1. Refinement statistics

Resolution (Å)	20–1.8
Non-H protein atoms	5059
Sulfates	4
Water	721
Reflection [completeness (%)][a]	67,970 (91/99)
R-factor (%)[b]	19.9 (27.0)
R_{free} (%)[b,c]	24.8 (31.1)
Average *B* (Å^2)	
Protein	25.8
Sulfate	30.5
Water	36.0
rmsd	
Bond lengths (Å)	0.011
Bond angles (°)	1.7

[a] Values for reflections with $F/\sigma(F) > 0.0$; the value for completeness for overall/high-resolution (1.87–1.80 Å) shell is in parentheses. Overall completeness is low due to removal of ice ring shells.

[b] Values for *R*-factor and R_{free} in the highest-resolution shell are shown in parentheses.

[c] R_{free} was calculated on the basis of 5% of the observed reflections that were randomly omitted from the refinement.

Fluorescence measurements

Fluorescence measurements, except for the [NaCl] titrations, were generally carried out in buffer T_{20} with BSA (otherwise indicated) at 25 °C using a PTI QM-4 fluorometer (Photon Technology International, Lawrenceville, NJ) equipped with a 75-W Xenon lamp. The slit widths were set at 0.5 mm for excitation and 1 mm for emission. The sample temperature in the cuvette was controlled using a Neslab RTE-111 recirculation water bath (Neslab, Newington, NH). The [NaCl] titrations were started in buffer T_{20} with no added NaCl (including BSA). The addition of BSA was necessary to prevent UvrD protein from sticking to the cuvette walls. Nonspecific sticking of BSA to the cuvette walls was monitored by the decrease in BSA Trp fluorescence with excitation at 295 nm and emission at 336 nm. The cuvette was placed in a thermostatted sample holder and equilibrated by constant stirring with a magnetic stirrer for at least 1 h. When the Trp fluorescence of BSA reached a constant value, the double-labeled UvrD mutant was added to a final concentration of 20 nM, and the fluorescence signal was measured after an additional 30-min equilibration. Fluorescence emission measurements using excitation/emission wavelengths of 515 nm/566 nm, 515 nm/670 nm and 620 nm/670 nm were made to obtain the donor fluorescence, the acceptor fluorescence and the acceptor fluorescence without energy transfer as an internal control, respectively. For titration experiments, the solution was allowed to equilibrate with stirring for 10 min after each addition of titrant. For each fluorescence measurement, the sample was excited for 15 s with an integration time of 2 s so that eight data points were taken, after which the shutter was closed. Fluorescence measurements were repeated every 2–3 min until the signal was constant. Data points from three measurements were averaged to obtain the final fluorescence. Stirring was maintained at a constant speed throughout each experiment. FRET occurs between two dyes when the emission spectrum of an excited donor fluorophore overlaps the absorption spectrum of a nearby acceptor fluorophore. FRET efficiency, *E*, depends on the inverse sixth power of the intermolecular separation, $E = R_0^6/(R^6 + R_0^6)$, where R_0 is the Förster radius (defined as the distance between donor and acceptor when $E = 50\%$). The donor–acceptor pair used here (Cy3/Cy5) has a Förster radius R_0 of 54 Å.[35]

Accession number

Coordinates and structure factors of apo UvrD have been deposited in the PDB with accession number 3LFU.

Supplementary materials related to this article can be found online at doi:10.1016/j.jmb.2011.06.019

Please cite this article as: Jia, H. *et al.*, Rotations of the 2B Sub-domain of *E. coli* UvrD Helicase/Translocase Coupled to Nucleotide and DNA Binding, *J. Mol. Biol.* (2011), doi:10.1016/j.jmb.2011.06.019

Acknowledgements

This work was supported in part by the National Institutes of Health (GM045948 to T.M.L., GM065367 to T.H. and GM073837 to S.K.). We thank T. Ho for synthesis and purification of the DNA and R. Galletto and E. Antony for discussions and comments on the manuscript.

References

1. Lohman, T. M. & Bjornson, K. P. (1996). Mechanisms of helicase-catalyzed DNA unwinding. *Annu. Rev. Biochem.* **65**, 169–214.
2. Singleton, M. R., Dillingham, M. S. & Wigley, D. B. (2007). Structure and mechanism of helicases and nucleic acid translocases. *Annu. Rev. Biochem.* **76**, 23–50.
3. Patel, S. S. & Picha, K. M. (2000). Structure and function of hexameric helicases. *Annu. Rev. Biochem.* **69**, 651–697.
4. Lohman, T. M., Tomko, E. J. & Wu, C. G. (2008). Non-hexameric DNA helicases and translocases: mechanisms and regulation. *Nat. Rev., Mol. Cell Biol.* **9**, 391–401.
5. Berger, J. M. (2008). SnapShot: nucleic acid helicases and translocases. *Cell*, **134**, 888–888.e1.
6. Gorbalenya, A. E. & Koonin, E. V. (1993). Helicases: amino acid sequence comparisons and structure–function relationships. *Curr. Opin. Struct. Biol.* **3**, 419–429.
7. Yamaguchi, M., Dao, V. & Modrich, P. (1998). MutS and MutL activate DNA helicase II in a mismatch-dependent manner. *J. Biol. Chem.* **273**, 9197–9201.
8. Husain, I., van Houten, B., Thomas, D. C., Abdel-Monem, M. & Sancar, A. (1985). Effect of DNA polymerase I and DNA helicase II on the turnover rate of UvrABC excision nuclease. *Proc. Natl Acad. Sci. USA*, **82**, 6774–6778.
9. Flores, M. J., Bidnenko, V. & Michel, B. (2004). The DNA repair helicase UvrD is essential for replication fork reversal in replication mutants. *EMBO Rep.* **5**, 983–988.
10. Payne, B. T., van Knippenberg, I. C., Bell, H., Filipe, S. R., Sherratt, D. J. & McGlynn, P. (2006). Replication fork blockage by transcription factor–DNA complexes in *Escherichia coli*. *Nucleic Acids Res.* **34**, 5194–5202.
11. Bruand, C. & Ehrlich, S. D. (2000). UvrD-dependent replication of rolling-circle plasmids in *Escherichia coli*. *Mol. Microbiol.* **35**, 204–210.
12. Flores, M. J., Sanchez, N. & Michel, B. (2005). A fork-clearing role for UvrD. *Mol. Microbiol.* **57**, 1664–1675.
13. Bidnenko, V., Lestini, R. & Michel, B. (2006). The *Escherichia coli* UvrD helicase is essential for Tus removal during recombination-dependent replication restart from Ter sites. *Mol. Microbiol.* **62**, 382–396.
14. Veaute, X., Delmas, S., Selva, M., Jeusset, J., Le Cam, E., Matic, I. *et al.* (2005). UvrD helicase, unlike Rep helicase, dismantles RecA nucleoprotein filaments in *Escherichia coli*. *EMBO J.* **24**, 180–189.
15. Lestini, R. & Michel, B. (2007). UvrD controls the access of recombination proteins to blocked replication forks. *EMBO J.* **26**, 3804–3814.
16. Delagoutte, E. & von Hippel, P. H. (2002). Helicase mechanisms and the coupling of helicases within macromolecular machines. Part I: structures and properties of isolated helicases. *Q. Rev. Biophys.* **35**, 431–478.
17. Byrd, A. K. & Raney, K. D. (2006). Displacement of a DNA binding protein by Dda helicase. *Nucleic Acids Res.* **34**, 3020–3029.
18. Dillingham, M. S., Wigley, D. B. & Webb, M. R. (2000). Demonstration of unidirectional single-stranded DNA translocation by PcrA helicase: measurement of step size and translocation speed. *Biochemistry*, **39**, 205–212.
19. Brendza, K. M., Cheng, W., Fischer, C. J., Chesnik, M. A., Niedziela-Majka, A. & Lohman, T. M. (2005). Autoinhibition of *Escherichia coli* Rep monomer helicase activity by its 2B subdomain. *Proc. Natl Acad. Sci. USA*, **102**, 10076–10081.
20. Fischer, C. J., Maluf, N. K. & Lohman, T. M. (2004). Mechanism of ATP-dependent translocation of *E. coli* UvrD monomers along single-stranded DNA. *J. Mol. Biol.* **344**, 1287–1309.
21. Cheng, W., Hsieh, J., Brendza, K. M. & Lohman, T. M. (2001). *E. coli* Rep oligomers are required to initiate DNA unwinding *in vitro*. *J. Mol. Biol.* **310**, 327–350.
22. Maluf, N. K., Fischer, C. J. & Lohman, T. M. (2003). A dimer of *Escherichia coli* UvrD is the active form of the helicase *in vitro*. *J. Mol. Biol.* **325**, 913–935.
23. Niedziela-Majka, A., Chesnik, M. A., Tomko, E. J. & Lohman, T. M. (2007). *Bacillus stearothermophilus* PcrA monomer is a single-stranded DNA translocase but not a processive helicase *in vitro*. *J. Biol. Chem.* **282**, 27076–27085.
24. Yang, Y., Dou, S. X., Ren, H., Wang, P. Y., Zhang, X. D., Qian, M. *et al.* (2008). Evidence for a functional dimeric form of the PcrA helicase in DNA unwinding. *Nucleic Acids Res.* **36**, 1976–1989.
25. Sun, B., Wei, K. J., Zhang, B., Zhang, X. H., Dou, S. X., Li, M. & Xi, X. G. (2008). Impediment of *E. coli* UvrD by DNA-destabilizing force reveals a strained-inchworm mechanism of DNA unwinding. *EMBO J.* **27**, 3279–3287.
26. Slatter, A. F., Thomas, C. D. & Webb, M. R. (2009). PcrA helicase tightly couples ATP hydrolysis to unwinding double-stranded DNA, modulated by the initiator protein for plasmid replication, RepD. *Biochemistry*, **48**, 6326–6334.
27. Subramanya, H. S., Bird, L. E., Brannigan, J. A. & Wigley, D. B. (1996). Crystal structure of a DExx box DNA helicase. *Nature*, **384**, 379–383.
28. Velankar, S. S., Soultanas, P., Dillingham, M. S., Subramanya, H. S. & Wigley, D. B. (1999). Crystal structures of complexes of PcrA DNA helicase with a DNA substrate indicate an inchworm mechanism. *Cell*, **97**, 75–84.
29. Korolev, S., Hsieh, J., Gauss, G. H., Lohman, T. M. & Waksman, G. (1997). Major domain swiveling revealed by the crystal structures of complexes of *E. coli* Rep helicase bound to single-stranded DNA and ADP. *Cell*, **90**, 635–647.
30. Lee, J. Y. & Yang, W. (2006). UvrD helicase unwinds DNA one base pair at a time by a two-part power stroke. *Cell*, **127**, 1349–1360.
31. Lee, J. & Yang, W. (2006). UvrD helicase unwinds DNA one base pair at a time by a two-part power stroke. *Cell*, **127**, 1349–1360.
32. Rasnik, I., Myong, S., Cheng, W., Lohman, T. M. & Ha, T. (2004). DNA-binding orientation and domain

Please cite this article as: Jia, H. *et al.*, Rotations of the 2B Sub-domain of *E. coli* UvrD Helicase/Translocase Coupled to Nucleotide and DNA Binding, *J. Mol. Biol.* (2011), doi:10.1016/j.jmb.2011.06.019

conformation of the *E. coli* rep helicase monomer bound to a partial duplex junction: single-molecule studies of fluorescently labeled enzymes. *J. Mol. Biol.* **336**, 395–408.
33. Park, J., Myong, S., Niedziela-Majka, A., Lee, K. S., Yu, J., Lohman, T. M. & Ha, T. (2010). PcrA helicase dismantles RecA filaments by reeling in DNA in uniform steps. *Cell*, **142**, 544–555.
34. Fischer, C. J. & Lohman, T. M. (2004). ATP-dependent translocation of proteins along single-stranded DNA: models and methods of analysis of pre-steady state kinetics. *J. Mol. Biol.* **344**, 1265–1286.
35. Ha, T., Rasnik, I., Cheng, W., Babcock, H. P., Gauss, G. H., Lohman, T. M. & Chu, S. (2002). Initiation and re-initiation of DNA unwinding by the *Escherichia coli* Rep helicase. *Nature*, **419**, 638–641.
36. Graham, D. L., Lowe, P. N., Grime, G. W., Marsh, M., Rittinger, K., Smerdon, S. J. *et al.* (2002). MgF(3)(−) as a transition state analog of phosphoryl transfer. *Chem. Biol.* **9**, 375–381.
37. Myong, S., Rasnik, I., Joo, C., Lohman, T. M. & Ha, T. (2005). Repetitive shuttling of a motor protein on DNA. *Nature*, **437**, 1321–1325.
38. Tomko, E. J., Jia, H., Park, J., Maluf, N. K., Ha, T. & Lohman, T. M. (2010). 5′-Single-stranded/duplex DNA junctions are loading sites for *E. coli* UvrD translocase. *EMBO J.* **29**, 3826–3839.
39. Cheng, W., Brendza, K. M., Gauss, G. H., Korolev, S., Waksman, G. & Lohman, T. M. (2002). The 2B domain of the *Escherichia coli* Rep protein is not required for DNA helicase activity. *Proc. Natl Acad. Sci. USA*, **99**, 16006–16011.
40. Soultanas, P. & Wigley, D. B. (2000). DNA helicases: 'inching forward'. *Curr. Opin. Struct. Biol.* **10**, 124–128.
41. Aregger, R. & Klostermeier, D. (2009). The DEAD box helicase YxiN maintains a closed conformation during ATP hydrolysis. *Biochemistry*, **48**, 10679–10681.
42. Theissen, B., Karow, A. R., Kohler, J., Gubaev, A. & Klostermeier, D. (2008). Cooperative binding of ATP and RNA induces a closed conformation in a DEAD box RNA helicase. *Proc. Natl Acad. Sci. USA*, **105**, 548–553.
43. Runyon, G. T., Wong, I. & Lohman, T. M. (1993). Overexpression, purification, DNA binding, and dimerization of the *Escherichia coli* uvrD gene product (helicase II). *Biochemistry*, **32**, 602–612.
44. Wong, I., Chao, K. L., Bujalowski, W. & Lohman, T. M. (1992). DNA-induced dimerization of the *Escherichia coli* rep helicase. Allosteric effects of single-stranded and duplex DNA. *J. Biol. Chem.* **267**, 7596–7610.
45. Holbrook, J. A., Capp, M. W., Saecker, R. M. & Record, M. T., Jr. (1999). Enthalpy and heat capacity changes for formation of an oligomeric DNA duplex: interpretation in terms of coupled processes of formation and association of single-stranded helices. *Biochemistry*, **38**, 8409–8422.
46. Otwinowski, Z. & Minor, W. (1997). Processing of X-ray diffraction data collected in oscillation mode. *Methods Enzymol.* **276**, 307–326.
47. Collaborative Computational Project, Number 4. (1994). The CCP4 suite: programs for protein crystallography. *Acta Crystallogr., Sect. D: Biol. Crystallogr.* **50**, 760–763.
48. Navaza, J. (1994). AMoRe: an automated package for molecular replacement. *Acta Crystallogr., Sect. A: Found. Crystallogr.* **50**, 157–163.
49. Brunger, A. T., Adams, P. D., Clore, G. M., DeLano, W. L., Gros, P., Grosse-Kunstleve, R. W. *et al.* (1998). Crystallography & NMR system: a new software suite for macromolecular structure determination. *Acta Crystallogr., Sect. D: Biol. Crystallogr.*, **54**, 905–921.
50. Jones, T. A., Zou, J. Y., Cowan, S. W. & Kjeldgaard, M. (1991). Improved methods for building protein models in electron density maps and the location of errors in these models. *Acta Crystallogr., Sect. A: Found. Crystallogr.* **47**, 110–119.
51. Murshudov, G. N., Vagin, A. A. & Dodson, E. J. (1997). Refinement of macromolecular structures by the maximum-likelihood method. *Acta Crystallogr., Sect. D: Biol. Crystallogr.* **53**, 240–255.

Please cite this article as: Jia, H. *et al.*, Rotations of the 2B Sub-domain of *E. coli* UvrD Helicase/Translocase Coupled to Nucleotide and DNA Binding, *J. Mol. Biol.* (2011), doi:10.1016/j.jmb.2011.06.019